Single-Nucleus Neuronal Transcriptional Profiling of Male *C. elegans* Uncovers Regulators of Sex-Specific and Sex-Shared Behaviors

Katherine S. Morillo[1, 2], Jonathan St. Ange[1, 2], Yifei Weng[1, 2], Rachel Kaletsky[1, 2], and Coleen T. Murphy[1, 2]*

Affiliations:

[1]Department of Molecular Biology, Princeton University; Princeton, NJ 08544, USA

[2]LSI Genomics, Princeton University; Princeton, NJ 08544, USA

*Corresponding author.

Email: ctmurphy@princeton.edu

Summary

Sexual differentiation of the nervous system causes differences in neuroanatomy, synaptic connectivity, and physiology. These sexually-dimorphic phenotypes ultimately translate into profound behavioral differences. *C. elegans'* two sexes, XO males and XX hermaphrodites, demonstrate differences in neurobiology and behavior. However, the neuron class and sex-specific transcriptomic differences, particularly at the single-neuron level, that cause such phenotypic divergence remains understudied. Here, using single-nucleus RNA sequencing, we assessed and compared adult male and hermaphrodite *C. elegans* neuronal transcriptomes, identifying sex-specific neurons, including previously-unannotated male neurons. Sex-shared neurons displayed large expression differences, with some neuron classes clustering as distinct neurons between the sexes. Males express ~100 male-specific GPCRs, largely limited to a subset of neurons. We identified the most highly-divergent neurons between the sexes, and functionally characterized a sex-shared target, *vhp-1,* in male-specific pheromone chemotaxis. Our data provide a resource for discovering nervous-system-wide sex transcriptomic differences and the molecular basis of sex-specific behaviors.

Keywords: neuronal single-nucleus sequencing, males, adult neurons, chemosensory GPCR, peptidergic GPCR, neuropeptides, AWC neurons, learning and memory, *C. elegans*

Introduction

Across sexually reproducing species, including flies, mice, and humans[1–3], biological sex impacts neuronal and cognitive function at multiple levels. Sexual dimorphic differences in cell number, gene expression, neuronal connectivity, and synaptic signaling result in differences in behavior and disease progression between the sexes. Yet most studies centered on neuronal biology and function using model organisms typically focus on one sex[4–6] or early developmental stages before the onset of many of these dimorphisms upon sexual maturation[7].

Caenorhabditis elegans has two sexes, hermaphrodites (XX) and males (XO)[8]. Both sexes have an invariant cell lineage and fully mapped connectomes[9]. Hermaphrodites have 8 sex-specific neurons, while males have 93 sex-specific neurons that are largely involved in male copulation behaviors[10]. The two sexes share 294 neurons, but many exhibit sexually dimorphic structural and functional features, such as differences in synaptic connectivity[8 9] and behavior (foraging, pheromone sensing, learning, and memory)[11–14]. Many of these behavioral differences are mediated by sex-specific regulation in a small subset of neurons[15,16]. Thus, identifying changes at the single-cell level is crucial to characterize the neuronal transcriptome and corresponding sexually dimorphic behaviors.

Bulk RNA-sequencing has been used to characterize the neuronal transcriptomes of both sexes throughout early development[17] and in young and aged male neurons[18], revealing extensive transcriptional variation between the sexes. However, while single-neuron transcriptional information exists for the L4 larval[7] and adult hermaphrodite[19], the male adult single-nucleus neuronal transcriptome remains undescribed. We set out to fill this gap by using single-nucleus RNA-sequencing to describe the transcriptome of adult male neurons. By developing a filtering technique and combining this with our previously-developed single-nucleus RNA sequencing pipeline for adult *C. elegans*, we were able to assess the neuronal transcriptome of young adult males, and then carry out comparisons with young adult hermaphrodites to identify sex-specific differences in neuronal transcription.

Results

High-throughput isolation of *C. elegans* males

Only ~0.1% of *C. elegans* are males; therefore, to obtain the large number of males required for single-nucleus RNA sequencing (snSeq), we crossed pan-neuronal histone-GFP-labeled hermaphrodites[19] into a *him-8* mutant background, which produces ~40% males[20]. We observed clear labeling of nuclei, including a high number in the tail where >70% of male neurons are expressed (Fig. 1A).

Day 1 of adulthood is marked by the onset of sexual maturity in *C. elegans;* both males and females start responding to mating cues at this stage[21]. Additionally, male-specific neurons, such as the MCM and PHD neurons, arise upon sexual maturation[22,23]. Using custom filters (Methods) to separate Day 1 adult males from Day 1 adult hermaphrodites, which are twice the size, we isolated ~95% pure populations of each sex (Fig. 1B).

Neuronal single-nucleus RNA sequencing of day 1 adult males

Single-nucleus RNA sequencing avoids RNA leakage caused by axon breakage in traditional cell isolation protocols, thus preserving transcripts in the nucleus[19]. We used our previously-developed method[19] to isolate and sequence adult *C. elegans* neuronal nuclei from filtered day 1 adult pan-neuronal histone-GFP tagged males, in parallel with nuclei from age- and genotypically-matched hermaphrodites. We used mechanical and chemical lysis to obtain a suspension of nuclei, Hoescht stained the nuclei, and then FACS sorted for both GFP and Hoescht signal (Fig. 1C, Methods). RNA was isolated, sequenced, and processed with Cell Ranger, ambient RNA was removed, and quality control metrics were assessed (Fig. S1). In total, we collected four male biological replicates and obtained 61,469 male neuronal nuclei after quality control, with an average median of 401 UMIs/nucleus and 298 genes/nucleus (Table S1).

C. elegans males have 387 neurons; 294 are shared between both sexes, and are grouped into 116 neuron classes based on similarities in morphology and connectivity[24], while 93 male-specific neurons fall into 27 classes[25]. To determine the male-specific neurons that were represented in our 110 clusters, we used a systematic and manual curation approach, as well as novel markers obtained from our previous adult wild-type hermaphrodite single nucleus dataset (Methods). Through this approach and additional refinements, we identified 108 of the 116 shared classes and 12/27 male-specific classes, successfully annotating >60% of the male clusters (Fig. 1D, Table S2). To assess how well our approach captured small subsets of well-characterized male-specific neurons, we examined the extracellular vesicle-releasing CEM, HOB, and ray neurons (Fig. 1E), which play a role in male mating behaviors[26]. We observed robust expression of polycystin/*pkd-2,* which is required for male sex drive in all these neuron classes, and enrichment of neuropeptide *flp-17* in rays 1, 5, and 7, as previously described[26] (Fig. 1E). Lectin/*clec-164,* which also regulates male sex drive[26], was also expressed in both CEM and ray neurons. Thus, our data reflect known male neuronal biology, allowing us to proceed in describing previously uncharacterized neurons.

Validation of male-specific clusters

To identify previously-uncharacterized male-specific clusters, we identified genes that were expressed either exclusively or in a limited subset of clusters of interest (Table S4). We annotated each cluster by generating promoter::GFP reporters and determining the expression profiles combined with neuron positional information. For example, the uncharacterized serpentine receptor *srd-66* was solely expressed in one of the unannotated clusters (Fig. 2A); *Psrd-66::GFP* is expressed in the male ventral cord, positionally indicative of the male CA7 neuron, with no observable expression in hermaphrodites (Fig. 2B). Furthermore, *eat-4,* which is expressed in CA7,[27] was also enriched in this cluster (Table S4), while *unc-47* (CP7 neuron) is not expressed (Table S4). Therefore, we are confident in our annotation of this cluster as male CA7 (Fig. 2A, B).

We were also able to identify all three male spicule neurons (SPC, SPV and SPD), which clustered separately (Fig. 1D, Table S2). The serpentine receptor *srh-217* was highly enriched in

male SPC neurons (40-fold higher expression relative any other neuron, Fig. 2C, D, Table S4), and we confirmed expression in the ASJ and AIB in both males and hermaphrodites (Fig. S2A), as was previously shown for hermaphrodites[7] (Fig. 2D; Table S4). We also observed expression of *srh-217* in hermaphrodite PHB neurons, as previously reported, but not in males, which correlates with our male expression data[7,19] (Fig. 2D). The serpentine receptor *srg-1* was highly enriched in the male SPD and SPV neurons, which have clear processes running down the length of the spicule shaft (Fig. 2E, F), but is only expressed in hermaphrodites in ASK chemosensory neurons, as previously reported[7,19]. Additionally, SPV and SPD but not SPC[28] express serpentine receptor *sra-1,* while *eat-4* is expressed in SPV, but not in SPD, as previously described[27]. Together, these data support our annotation of the three male spicule neurons.

Identification of the PHD as chemosensory neurons

The PHD neurons are a recently-discovered neuron pair that arise from a glia-to-neuron cell fate switch upon sexual maturation, resulting in cholinergic, likely peptidergic ciliated neurons that may also be proprioceptive[29]. The PHD neurons were identified among the unannotated clusters using a GFP reporter for *srt-18*, which was highly enriched in a single cluster (Fig. 2G, Table S4). *Psrt-18::GFP* was expressed in a pair of neurons in the male tail whose morphology and location near the lumbar ganglia most closely resembles the male PHD ciliated sensory neurons[29] (Fig. 2H). The PHD cluster expresses ciliated neuron markers (*dyf* and *osm* genes) (Table S5), indicating a ciliated sensory neuron, and the IG domain containing protein, *oig-8,* which is highly expressed in the PHD[23], is also enriched (Table S4). Additionally, the phogrin ortholog *ida-1* (dense-core vesicle secretion[23,30]) and >45 neuropeptide genes, including the highest-expressed neuropeptide, *nlp-50*, are highly expressed, along with the vesicular acetylcholine transporter *unc-17,* congruent with PHD peptidergic activity and cholinergic neurotransmission. The transcriptome of this *srt-18* male cluster is enriched for genes related to ion channel activity, signal transduction, response to stimulus, and localization, further suggesting the sensory function of these neurons (Fig. 2I). Together, these data provide strong evidence that this cluster represents the recently-discovered male PHD neurons.

Intriguingly, the chemoreceptor for female volatile sex pheromone, *srd-1,* was not only highly expressed in AWA and ASI as previously reported,[31] but was also expressed in >40% of cells of the PHD neuron cluster (Table S4), suggesting the PHD might have a role in pheromone sensing. Indeed, knockdown of *srt-18* in adult males reduces their ability to respond to female pheromones (Fig. 2J). Together, these findings suggest this new neuron class, in a distinct anatomical location, may mediate pheromone sensing, unveiling a previously undescribed chemosensory function.

Hierarchical clustering reveals functional relationships and sex-specific features

A transcriptome-based dendrogram of hierarchically clustered male neurons (Fig. 2K) revealed that most neurons group by type (chemosensory, motor, etc.) as expected, with

transcriptomic-based dendrograms reflecting functional similarities that supersede lineages[19]. Male-specific neurons (e.g., CEM, HOB, and ray neurons) cluster together, and other associations aided in identifying previously unannotated neuron clusters (Fig. 1D). Hierarchical clustering also revealed associations specific to the male neuronal transcriptome. For instance, the AWA, PHD, and SPV neurons clustered together. The SPV are putative chemosensory neurons[32] that are proposed to sense vulval pheromone and coordinate sperm release. The clustering of these three neurons further suggests a role for the PHD in chemosensory and male-behavior associated functions.

One unannotated male-biased cluster was highly enriched for ciliated neuron markers and for the serpentine receptor *srg-14* (Fig. 2L), which is also expressed in URX, AQR, PQR, and ASJ[28] (Table S4, S5). Hierarchical clustering and other tests indicated that this cluster was most similar to PHA and PHB sensory neurons (Fig. 2K, Table S2). *Psrg-14::GFP* was highly expressed in at least 6 cell bodies in the male tail (Fig. 2M; Fig. S1). Together, these data suggest this neuronal cluster corresponds to sexually dimorphic PHA and PHB neurons, which play a role in male mate-searching behavior and have dimorphic connections to downstream interneuron partners[32,33].

Male-specific target genes correlate with male behaviors

To find male-specific genes, we identified genes expressed in our male dataset that were not expressed in at least one cell type at the most stringent threshold in our previous wild-type adult hermaphrodite snSeq dataset[19], resulting in a list of 693 genes, including 591 neuron-specific genes (Table S6). Many of the genes on this “male specific” list are not well characterized apart from associations with cellular components. These genes were enriched for signal transduction-related functions, such as G protein-coupled receptor and phosphoprotein phosphatase activity (Fig. 3A, Table S6). 7% of these genes are C-type lectins; while C-type lectins are present in the vas deferens[35], a distinct set of *clec* genes are expressed in CEM, HOB, and ray neurons (Fig. 3B, Table S7) and may mediate male mating efficiency[8,26,35].

G protein-coupled receptors (GPCRs) directly respond to environmental stimuli by binding to a variety of molecules, from odorants to neuropeptides[36]. The *C. elegans* genome encodes roughly 1500 GPCRs, of which 1341 are chemosensory GPCRs[28]. These csGPCRs respond to pheromones, food-related cues, and repellents, driving behaviors like foraging and mate searching. We surveyed the expression of 98 csGPCRs that were expressed in adult neurons of males but not hermaphrodites. Some, such as *srd-58* (ADF) and *srx-78* (PHA/PHB) are strong cell-specific markers. Notably, we captured known male-specific GPCRs such as *sra-1*[28] (SPV and SPD), *srr-7* (male CEM, HOB, and ray neurons[26]), and *srd-66,* which is expressed in the male CA7 neuron (Fig. 2A,3 C, Table S4,S8). Some of these csGPCRs showed similar expression patterns in males as previously observed in larval hermaphrodites (e.g., *str-256* in AWA and *srh-37* in ASK[39]). Others showed sex-specific expression patterns: *srv-25* was expressed in PHA/PHB (Fig. 3C) and male CP9 (Table S4), but is highly expressed in ASJ only in L4 hermaphrodites[7] but not in adult hermaphrodites[19]. Similarly, *srh-300* was expressed in male ASH neurons, but was only previously shown to be enriched in larval stage, but not adult[19],

hermaphrodite AVE[38] and AVK[39] neurons. *srw-87,* which was enriched in young male neurons and previously shown to be expressed in ADF at the embryonic stage[40], was solely expressed in the male ADF neurons in our data. Collectively, these data demonstrate the variability in expression stemming from different sexes and developmental stages.

The expression of these male-only GPCRs also illuminates possible functional insights. First, male-specific neurons such as SPV and SPD have several GPCRs in common, consistent with their homologous functional roles (Fig. 3C, Table S8). The majority of these male-specific GPCRs are expressed in chemosensory neurons that are shared between the sexes, such as PHA/PHB, AWA, ADF, and ASK (Fig. 3C). All these neurons have known roles in male sex drive and mating behaviors. For example, PHA, along with URY and PQR, regulates male reproductive drive through PDF-1 neuropeptide signaling[33]. The sex of the ADF neuron determines an animal's response to pheromone[15], and the ASK neurons directly sense ascaroside sex pheromones[41]. Thus, the candidates provided here may present additional components in the pathways driving these male behaviors.

Heterogeneity of sex-shared molecular machinery

In addition to uncovering sex-specific targets, we wanted to better understand how each of the sexes employs the same molecular machinery to regulate divergent phenotypic outcomes. Of the csGPCRs that were expressed in at least 1% of cells and in at least one cluster in both sexes, the majority show similar expression patterns, i.e., if a csGPCR was expressed in males in a particular neuron class, it was also expressed in the same neurons in hermaphrodites (Fig. 3D, Table S8). However, there were multiple examples of sex-specific expression within a given neuron, or heterogeneity in expression of the same GPCR across different cell types between the sexes. For example, *sra-37* was detected in ASER and ADF in both sexes, but was hermaphrodite-specific in AWC, ASI, and ASK, and male-specific in ASEL. Chemosensory neurons ADL, ASJ, and ADF show highest expression of male-biased GPCRs.

The *C. elegans* genome contains over 100 neuropeptide-coding genes. Neuropeptides modulate many sex-shared and specific behaviors in *C. elegans,* such as feeding, learning, and reproduction[42–44]. The two major types of neuropeptides are the FMRFamide-related peptides (FLPs) and the neuropeptide-like proteins (NLPs)[45,46]. We find 104 FLP or NLP neuropeptides shared between male and hermaphrodite[19] neurons when comparing across the same threshold (Table S8). *flp-1* and *flp-8* (hermaphrodite) and *nlp-43* and *flp-34* (male) are examples of sex-biased neuropeptides. The subset of interneurons with the highest incidence of sex-shared neuropeptides in our male dataset include PVS (PVP in hermaphrodites), AIY, RMH, AVA, AWB, and URA neurons (Fig. 3E). PVS expressed the highest number of neuropeptides in males, with several male-enriched neuropeptides, while the AUA displays a high prevalence of hermaphrodite-enriched neuropeptides.

snSeq reveals extensive sexually-dimorphic neurons and sex-divergent functional roles

To further characterize sex-specific differential expression, we integrated the male and genotypically-matched *him-8* hermaphrodite datasets, including 46,685 hermaphrodite neuronal nuclei (Table S10). After processing and unsupervised network clustering of the quality controlled and normalized data, obtained 145 clusters, annotating 108 of 116 shared neurons classes (Fig. 4A).

We further examined the contribution of nuclei from each sex and biological replicates per cluster (Fig. 4B). Sex-specific neurons, such as the CEM and ray in males and the HSN and VC neurons in hermaphrodites, were >95% enriched for nuclei of the corresponding sex. In fact, some sex shared neurons were so dimorphic they cluster as separate cell types. For example, although the homologous gene expression and functional roles of CEP, ADE, and PDE - which comprise 8 sex-shared dopaminergic neurons with mechanosensory functions[24] - cause them to cluster together, the sex-specific differences in expression cause the cluster to diverge. Similarly, the URA/URY neurons form a single cluster in hermaphrodites, but two distinct male clusters (Fig. 4B, Table S3). Signaling-related genes, including neuropeptides (e.g., *nlp-45*, *flp-4, nlp-11, flp-6, nlp-64*), receptors (*dmsr-2, pdf-1, ser-7*), and signaling genes (*kcc-2, snet-1*), are enriched in male neurons in these extensively dimorphic clusters (Fig. 4C; Table S11).

Next, to identify the neurons with the largest differences between the sexes, we calculated the Euclidean distance between male and hermaphrodite neurons (Table S12, Fig. 4D). For this analysis, we only considered “sex-shared” clusters as marked by >30% nuclei from each sex present within the corresponding cluster. (The AWA neurons are an exception to this threshold as they are made up of 72% male nuclei (Table S3), suggesting that the male AWA may be easier to isolate than its hermaphrodite counterpart.) The AIM, AVG, and AVF were the most divergent interneurons, the VB/DB/SAB and PDA were the most divergent motor neurons, and the AWA, PHA/PHB, AWA, and ADF were the most distant chemosensory neurons between males and hermaphrodites. Mechanosensory sensory neurons, encompassing touch neurons such as ALM and PLM, also showed high sex divergence.

We assessed the differentially-expressed genes between the sexes in these clusters. We confirmed that the food chemoreceptor *odr-10* is solely expressed in the AWA chemosensory neurons[47], and its relative upregulation in hermaphrodites relative to males[16] (Fig. 4E, S3A). Similarly, we confirmed the upregulation of the canonical pheromone receptor[31] *srd-1* in male AWA (Fig. S3B). Overall, most differentially-expressed genes across neurons were downregulated in males (Table S14). Thus, we posited that genes upregulated in males, like *srd-1,* may identify uncharacterized targets and their functional roles. Male upregulated genes include chemosensory and peptidergic GPCRs, neuropeptides, ion channels, and enzymes (Fig. 4F,G, Table S14). There was a global enrichment of ion channels, including *kcnl-1, kcnl-2, egl-23,* and *egl-26.* Over 100 genes were upregulated in the memory-associated AIM in males (Fig. 4G, Table S14).

While most genes exhibited neuron-specific increased expression, the MAPK phosphatase *vhp-1* was expressed at higher levels in males in several neurons (ASK, ASJ, and AVF) (Fig. 4F-H, Fig. S3C, Table S14). Since ASK neurons play a role in pheromone sensing[41] and are one of three core neurons required for sexual attraction in males, we hypothesized that *vhp-1* may play a role in pheromone sensing. We used neuron-specific RNAi to knock down *vhp-1* and

assayed males' ability to chemotaxis to female pheromone; pheromone chemotaxis was robust attenuated (Fig. 4I). Thus, *vhp-1*, a MAPK enriched in males in several extensively sexually-dimorphic neurons, mediates male-specific behavior.

DISCUSSION

Here, we used snSeq to characterize the adult male neuronal transcriptome. After confirming previously characterized neurons, we combined various approaches - including comparison with our previous snSeq hermaphrodite dataset - to annotate previously-uncharacterized male-specific neurons, including the male PHD and spicule neurons. We then surveyed the chemosensory GPCRs (csGPCRs) in both sexes and found that males express roughly 100 male-specific csGPCRs; most of these were present in a limited subset of sex-shared chemosensory neurons. We also observe heterogeneity in expression in GPCRs shared between the sexes, as well as sex-shared neuropeptides. Some differences in the sex-shared neurons were so extreme that they cause divergent clustering of similar cell types. These divergent neurons include the sex-shared dopaminergic neurons. Among the sex-shared neurons, several are quite distant between the sexes, including specific chemosensory neurons. We also identified highly sex-divergent interneurons, with the AIM interneurons displaying the most divergence. Lastly, through the sex-specific lens used in this study, we identified candidates such as *vhp-1/*MAPK phosphatase*,* which was upregulated in specific male neurons, leading to the discovery that *vhp-1* is required for pheromone sensation.

Heterogeneity in gene expression exists across sex-shared and sex-specific neurons. We characterized the transcriptional landscape of the recently discovered male PHD sensory neurons. Our data suggest these neurons are similar in expression profile to the shared AWA chemosensory neurons, which express one of the only known chemoreceptors for volatile sex pheromone[31], *srd-1,* along with other adult male-specific GPCRs*.* The AWA and male PHD neurons share many genes related to chemosensory functions, including neuropeptides, csGPCRs, peptidergic GPCRs, and ion channels, such as *ocr-1.* OCR-1 is a transient receptor potential vanilloid (TRPV) channel that acts a temperature sensor in AWA, thus may play a similar role in the male PHD neurons or mediate proprioception in this novel class. Intriguingly, *ocr-1* is also upregulated in male AWA neurons compared to hermaphrodites. The human OCR-1 ortholog, TRPV2, is critical for mechanical nociception in the adult somatosensory system[48]. Additionally, differential regulation of these TRP channels between the sexes has been linked to higher prevalence of chronic pain seen in females compared to their male counterparts[49].

We compared our findings to our hermaphrodite neuronal expression to identify sexually conserved and dimorphic neuronal expression. We identified many dimorphically-expressed genes, including GPCRs, neuropeptides, ion channels, and C-type lectins. Using single-cell analysis, we uncovered highly-dimorphic shared neurons between the sexes that cluster into separate cell types. Lastly, through functional validation of differentially expressed targets in these and other highly dimorphic neurons, we were able to link transcriptional data with effects on behavior. For example, our behavioral data supported hypotheses regarding the roles of both *srt-18* and *vhp-1* in male chemotaxis to female pheromone.

These are a few of many possibly examples where we capture novel sex-specific features in *C. elegans* and conserved differential expression patterns that may influence neurological function and behavior. This atlas of adult male neurons provides transcriptional information for sex-specific and shared *C. elegans* adult male neurons, offering candidate cell markers and gene expression data that will facilitate the study of male and sex differences in future efforts.

Resource availability

Lead contact

Further information and requests will be fulfilled by the lead contact, Coleen T. Murphy (ctmurphy@princeton.edu).

Materials availability

Strains generated in this study are available upon request. This study did not generate new unique reagents.

Data and code availability

Single-nucleus RNA-seq data have been deposited at NCBI and are publicly available as of the date of publication (BioProject PRJNA1195922). All other data are available in the main text or supplementary material. Any additional information required to reanalyze the data reported in this paper is available from the lead contact upon request.

Acknowledgments:

We thank Christina DeCoste and Princeton FACS Core, Jennifer Miller, Jean Arly Vomar, Wei Wang, and the Princeton Genomics Core for their assistance, the *C. elegans* Genetics Center for strains, and members of the Murphy lab for suggestions on the manuscript.

Funding:

HHMI Gilliam Fellowship to KSM

The Simons Foundation (811235SPI) to CTM

China Scholarship Council (CSC) to YW

NSF GRFP to JSA (DGE-2039656)

NIH Office of the Director Pioneer Award to CTM (NIGMS DP1GM119167)

Author contributions:

Conceptualization: KSM, RK, JSA, YW, CTM

Methodology: KSM, RK, JSA, RK

Investigation: KSM, YW, JSA, RK

Visualization: KSM, JSA

Funding acquisition: CTM

Project administration: CTM

Supervision: RK, CTM

Writing – original draft: KSM

Writing – review & editing: KSM, RK, CTM

Declaration of interests: Authors declare that they have no competing interests.

Figure Legends

Figure 1: Single nucleus RNA sequencing of adult male *C. elegans* neurons. (A) Representative image of pan-neuronal GFP tagged *him-8* males (*Prgef-1::his-58::GFP;him-8)*. **(B)** 6-well tissue culture inserts with modified filters were used to separate sexes in *C. elegans,* achieving an average ~95% purity for both male and hermaphrodite fractions. **(C)** Overview of nuclei isolation and sequencing. Pan-neuronal histone GFP-tagged *him-8* males and hermaphrodites were separated, nuclei were isolated, FACS sorted for Hoescht and DAPI positive nuclei, followed by barcoding, cDNA amplification, and library preparation using 10X genomics chromium X, then Illumina RNA sequenced. **(D)** UMAP of 61,936 male-specific neurons that passed quality control. **(E)** Feature plot of *pkd-2, clec-164, flp-17,* and *Y70G10A.2* expression (known markers expressed in CEM, HOB, and ray neurons).

Figure 2: Validation of neuronal clusters. (A) Feature plot of *srd-66* expression. **(B)** Imaging of *srd-66p::GFP* shows corresponding expression and morphology for male CA7 neurons in day 1 adult males; expression is male-specific, as no signal was detected in age-matched hermaphrodites. **(C)** Feature plot of *srh-217* expression. **(D)** Imaging of *srh-217p::GFP* shows corresponding expression and morphology for male SPC neurons, and hermaphrodite-specific PHB expression as previously reported. **(E)** Feature plot of *srg-1* expression. **(F)** Imaging of *srg-1p::GFP* shows corresponding expression and morphology for male SPV and SPD neurons, and no expression in hermaphrodites. **(G)** Feature plot of *srt-18* expression. (**A, C, E, G**) Scale bar = SCT normalized expression level. **(H)** Imaging of *srt-18p::GFP* shows corresponding expression and location for male PHD neurons. We did not observe any signal in hermaphrodites (not shown). **(I)** Significant Gene Ontology (GO) terms for PHD-enriched genes (Bonferroni padj < 0.05). **(J)** Males' ability to chemotaxis to female pheromone is attenuated upon *srt-18* neuron-specific RNAi knockdown. Chemotaxis assay performed using males from TU3595 neuron-specific RNAi-sensitive strain. One biological replicate, 5 chemotaxis plates per replicate, ~30 worms per plate. *p<0.05. Unpaired, two-tailed Student's t-test. **(K)** Hierarchical dendrogram based on gene expression in each day 1 adult male neuron. Neurons are color-coded by functional subtype. Blue arrow indicates PHA/B cluster shown in (L). **(L)** Feature plot of s*rg-14* expression. (**M**) Imaging of *srg-14p::GFP* shows corresponding expression and neuronal morphology in hermaphrodite PQR in the tail, while we observe at least 6 cell bodies expressing reporter in the male tail.

Figure 3: Characterizing sex-specific and sex-shared targets indicates heterogeneous gene regulation between the sexes. (A) Gene Ontology (GO) terms associated with male-specific genes not detected in N2 hermaphrodite single-nucleus transcriptomic dataset at the least stringent threshold. GO terms generated using g:Profiler. **(B)** Expression of male-specific C-type lectins in vas deferens and male-specific neurons. Normalized average expression values and percentage of cells expressing the corresponding gene are shown. **(C)** Male-only csGPCRs are enriched in a subset of sensory neurons with known sexually dimorphic functions. Normalized average expression values and percentage of cells expressing the corresponding

gene are shown. **(D)** Heatmap of heterogeneity of sex-shared csGPCRs and **(E)** neuropeptide expression between sexes. Genes present in at least 1% of cells with an average expression >0.001 in at least one cell type. Genes expressed in the same cell type in both sexes are shown in gray. Those only in male are in blue and only in hermaphrodites are in red.

Figure 4. Sex-shared neurons reveal a highly dimorphic neuronal landscape. (A) UMAP of all 178,606 male and hermaphrodite nuclei that passed quality control, resulting in 145 distinct clusters. **(B)** Contribution of nuclei from each sex per cluster across biological replicates (4 male, 3 hermaphrodite). **(C)** Genes significantly higher in males in CEP/ADE/PDE and RMG neurons. Expression level density of male (blue) or hermaphrodite (red). Adjusted p-values from Wilcoxon Rank Sum test. **(D)** Euclidean distance of each neuron's mean male vector and mean hermaphrodite vector. The top neuron subtypes with the largest distance are shown. **(E)** Feature plot of *odr-10* expression and violin plot of *odr-10* differential expression between sexes. **(F)** Genes higher in males (blue) in selected highly distant chemosensory neurons and **(G)** interneurons between the sexes. **(H)** Expression level of *vhp-1* in ASK and ASJ in both sexes. **(I)** Knockdown of *vhp-1* in neuron RNAi-sensitive males impairs chemotaxis to *C. remanei* female pheromone. N= 3 biological replicates, 5-10 chemotaxis plates per replicate with ~10-30 worms per plate. Unpaired, two-tailed Student's t-test. *p<0.05. ****p<0.0001.

Supplementary Figure 1: Quality control metrics for single nucleus RNA-seq. **(A)** Number of cells across all replicates for each sex. **(B)** Number of UMIs per sex. **(C)** Number of genes per cell density. **(D)** Genes per UMI relative to cell density. **(E)** Number of genes relative to the number of UMIs across both sexes.

Supplementary Figure 2: (A) Imaging of *srh-217p::GFP* shows expression in ASJ and AIB in both males and hermaphrodites. **(B)** Merge image of brightfield, DsRed and GFP channel after DiI staining in day 1 hermaphrodites. DiI stains phasmid PHA and PHB and serves as reference point validating nearby location of PQR.

Supplementary Figure 3: (A) Feature plot of *odr-10* expression between the two sexes **(B)** Expression level of *srd-1* in AWA, upregulated in males. Adjusted p-values from Wilcoxon Rank Sum test**. (C)** Expression level of *vhp-1* in AVF, upregulated in males. ****p<0.0001.

STAR Methods

Resource availability

Lead contact

Further information and requests for resources and reagents should be directed to and will be fulfilled by the lead contact, Coleen T. Murphy (ctmurphy@princeton.edu).

Materials availability

Worm strains generated in this study are available upon request. This study did not generate new unique reagents.

Data and code availability

Single-cell RNA-seq data have been deposited at NCBI and are publicly available as of the date of publication. Accession number is PRJNA1195922 and is also listed in the key resources table. All other data are available in the main text or supplementary material. Any additional information required to reanalyze the data reported in this paper is available from the lead contact upon request.

C. elegans growth and maintenance

All strains were maintained at 20C using standard methods for the duration of experiments[50]. *C. elegans* were maintained on plates made with high growth medium (HG: 3 g/L NaCl, 20 g/L Bacto-peptone, 30 g/L Bacto-agar in distilled water) with 4 mL/L cholesterol (5 mg/mL in ethanol), 1 mL/L 1M CaCl2, 1 mL/L 1M MgSO4, and 25 mL/L 1M potassium phosphate buffer (pH 6.0) added to the autoclave media after it has cooled to < 60C. Plates were seeded with a full lawn of OP50 *E. coli* (From the CGC) for *ad libitium* feeding. For RNA interference assays, animals were grown on HG seeded with OP50 until L4, then transferred onto HG made with 1 mM IPTG, 100 mg/L Carbenicilin, and 50 uM Floxuridine (FuDR) seeded with respective HT115 RNAi bacteria from the Ahringer Library[51]until day 2. Day 2 animals were then transferred to plates without FuDR seeded with the respective freshly inoculated HT115 RNAi bacteria. All behavior assays were performed on plates made with standard nematode growth medium (NGM: 3 g/L NaCl, 2.5 g/L Bacto-peptone, 17 g/L Bactoagar in distilled water) with 1 mL/L cholesterol (5 mg/mL in ethanol), 1 mL/L 1M CaCl2, 1 mL/L 1M MgSO4, and 25 mL/L 1M potassium phosphate buffer (pH 6.0) added to the autoclave media after it has cooled to < 60C. Hypochlorite synchronization was used to developmentally synchronize experimental worms, where gravid hermaphrodites were exposed to an alkaline-bleach solution (e.g. 7.5 mL sodium hypochlorite, 2.5 mL KOH, 41.5 mL distilled water) to collect eggs, followed by repeated washes with M9 buffer (6 g/L Na2HPO4, 3 g/L KH2PO4, 5 g/L NaCl and 1 mL/L 1M MgSO4 in distilled water)[50].

C. elegans strains in this study

CQ760: *wqIs7 [Prgef-1::his-58::GFP] him-8(e1489) IV*

CQ830: *srd-66p::GFP;Pmyo3::mcherry (co-injection marker)*

CQ828*: srg-1p::GFP;Pmyo3::mcherry(co-injection marker)*

CQ854: *srh-217p::GFP;Pmyo3::mcherry(co-injection marker)*

CQ855: *srt-18p::GFP;Pmyo3::mcherry(co-injection marker)*

TU3595: *sid-1(pk3321) him-5(e1490) V; lin-15B(n744) X; uIs72 [pCFJ90(Pmyo-2::mCherry) + Punc-119::sid-1 + Pmec-18::mec-18::GFP]*

CQ826: *srg-14p::GFP;Pmyo3::mcherry(co-injection marker)*

PB4641: *C. remanei*

Filter design and efficiency testing

Adult males are shorter and more slender than hermaphrodites[52], thus we capitalized on this size difference to separate the sexes. We removed existing meshes from 6-well tissue culture inserts (CellQart, item#: 9300002) and replaced them with 35 µm nylon meshes (BioDesign Inc. of New York, CellMicroSieves, product #: N35S) adhered to the inserts with a very thin film of epoxy resin (Loctite, epoxy adhesive, EA015) used along the insert border. Inserts are dried overnight, meshes are cut to shape, then sterilized with ethanol. The ethanol is allowed to evaporate, and the inserts are washed with M9 before filtering animals. We tested the efficiency of each individual filter using ~200 µL of synchronized CQ760 hermaphrodites and males. We added 50 µL of animals to each individual filter and enough M9 to lightly submerge the animals. After visual inspection, each corresponding top and bottom fraction were then added to individual 15 mL conical tubes (8 total, 1 hermaphrodite- and 1 male-enriched tube/filter) and animals were allowed to settle. Then 5 µL of animals corresponding to each fraction was transferred to NGM plates seeded with 150 µL of OP50, animals were allowed to spread then paralyzed with 7.5 % sodium azide to facilitate counting. The number of males and hermaphrodites on half of each plate were counted. We then calculated the percent efficiency. It is important to note that filters may tear, decreasing their efficiency, but this is easily visualized upon inspection of 6-well plates under a standard microscope prior to downstream processing. Filter efficiency is calculated as follows:

$$\text{hermaphrodite fraction: } \frac{\#\text{ of hermaphrodites} - \#\text{ of males}}{Total}\ x\ 100$$

$$\text{male fraction: } \frac{\#\text{ of males} - \#\text{ of hermaphrodites}}{Total}\ x\ 100$$

Neuronal nuclei isolation

C. elegans neuronal nuclei were isolated as previously described[19] with minor modifications. About 0.8-1 mL of Day 1 synchronized hermaphrodites and males (CQ760) were washed from HG plates, then washed 3X times with M9 to get rid of excess OP50. Animals were then transferred to 6-well inserts with 35 µm nylon filters submerged in M9 to separate both sexes. We use 4 filters for each replicate. Roughly 150-200 µL of animals are added to each filter and

allowed to filter for ~5 min. Upon inspection of the top fraction (hermaphrodite-enriched) and bottom fraction (male-enriched), the respective fractions are pipetted into fresh 15 mL conical tubes for downstream nuclei isolation.

First, hermaphrodites were Dounce homogenized in lysis buffer 30-50x and males 50-90x to break open the cuticle. Briefly, after chemo-mechanical lysis, the pellet was resuspended in 500 µL wash buffer, Hoechst stained (1:10,000 dilution; Molecular Probes Hoechst 33342, Thermo Fisher, Cat. # H3570) was added to each sample, and samples were passed through 5 µm syringe filters, directly into FACS tubes. Samples were incubated for at least 5 min on ice prior to FACS.

Nuclei positive for both Hoechst and GFP+ were sorted using a 70 µm nozzle and a flow rate of 3 on a BD Biosciences FACSAria Fusion sorter into a 1.5 mL low bind microcentrifuge tube containing collection buffer (500 µL of 0.5% BSA + 1.5. U/µL RNase Inhibitor). The instrument was washed with bleach between samples. We performed 3 biological replicates for hermaphrodites and 4 biological replicates for males to increase the number of male nuclei. For the 4th male biological replicate samples were split into two technical replicates by splitting ~300 µL of filtered males into two aliquots and following all described downstream nuclei isolation steps.

snRNA-seq library preparation, sequencing, alignment, and data quality control

After FACS, samples were centrifuged gently at 1000 x g for 5 min at 4°C. The gentle speed, while important to keep the nuclei intact, leaves many of them behind in the supernatant. The supernatant was removed, and nuclei were resuspended in 20 µL of collection buffer. Single nuclei suspension samples were then provided to the Princeton Genomics Core for 10X Genomics Chromium X barcoding, cDNA amplification, library preparation and Illumina next generation sequencing, as described in St. Ange and Weng et al. 2024[19]. After Illumina sequencing, reads were aligned using CellRanger version 7.1.0. SoupX was used to remove ambient RNA contamination on Cell Ranger output files, and calculated contamination fractions were between 0.12 - 0.50 for all samples.

Next, we assessed quality control metrics to give us insight into the depth, complexity, and overall quality of our data. Average genes/cell, average UMIs/cell, and number of cells per cluster were all assessed. Violin Plots of genes per cell were generated to determine cutoffs: the lower bound was 100-300 features/cell for each sample (to remove damaged nuclei and empty droplets) and the higher bound was between 750 and 1500 features/nucleus (to remove doublets) depending on the sample. Data outside of these cutoffs were excluded from further analysis.

Normalization, Integration, and Clustering

We used the Seurat package single cell genomics pipeline for normalization, integration and clustering. We first merged all of the replicates. Next, we normalized the data using single cell

transform (SCT), which normalizes single cell data by fitting genes to a negative binomial distribution. We generated an elbow plot of the principal components (PCs) to determine the number of PCs to include in dimensional reduction, and we used the Louvain algorithm for unsupervised network clustering. We tested different resolutions: 0.6 - 2.4 in 0.2 intervals. Ultimately, we clustered the data using 150 PCs at a clustering resolution of 1.4. This resulted in 110 clusters for the male data processed on its own, and 145 clusters for the male and hermaphrodite data processed together.

General Cluster Labeling/Cell Type Analysis

Cluster annotation for the male-specific transcriptome was performed using a combination of systemic and manual approaches as described in St. Ange & Weng et al. 2024[19], with some additional curation used for understudied male-specific clusters. We first focused on only the male biological replicates to characterize the male transcriptome.

First, we used the 'FindAllMarkers' function in Seurat to identify cluster-specific markers. These markers corresponded to genes showing significant differential expression ($\log_2 FC > 0.25$) within each cluster compared to the average expression across all clusters and were expressed in >25% of cells in the corresponding cluster.

We then compared the identified cell markers to a curated list of known markers for each neuron type classification (Table S2). This list comes from existing sequencing data and literature. Two statistical tests were used for this comparison: 1) A hypergeometric test, assessing the Bonferroni-corrected p-value of the overlapping genes (genes present in both the cell markers list and the curated list). Clusters demonstrating a significant overlap ($p < 0.01$) with known anatomy markers were considered for the corresponding neuron type. 2) An Area-Under-the-Curve (AUCell) algorithm, which accounts for level of expression of a given gene set within the respective cell. Gene set lists were generated based on the known markers associated with a given neuron type and ranked by expression level in the cell in question. Using these rankings, we can calculate the AUC value of each gene set in each cell. To assign neuron types to cells, we generated a histogram of AUCell values and applied a threshold, manually adjusting the threshold in some cases to ensure approximately 5% of cells were assigned to each neuron term. Subsequently, we assembled these cells into clusters and determined the percent assigned to each neuron type. Neuron types with the highest 10 percentages were assessed for annotation. The agreement of these two statistical tests allows us to annotate clusters with neuronal identities in an unbiased way.

To add confidence to our annotations, we performed the hypergeometric test on not only the curated list, but also using the neuron type markers reported by St. Ange & Weng et al. 2024[19]. To annotate a given cluster, we used the results from the two hypergeometric tests, and the AUCell algorithm. If all three methods aligned, we regarded this as the final annotation. In case of disagreement, we examined gold-standard markers associated with that neuron and made a manual decision.

Annotation of Male Specific Neurons

For most male-enriched neurons (>70% nuclei stemming from a male sample when clustered with hermaphrodite biological replicates), markers are sparse, thus the statistical tests rarely reflect neuronal identity. First, we chose markers in our data that appeared cluster specific to generate fluorescent reporters to inform neuronal annotation. In instances where a male-enriched neuron could not be annotated through statistics or fluorescent reporters, it was labeled as closely to its neuron class as we could: male inter/motor "x"/male sensory. The results of both mechanisms and the final annotation are summarized in supplemental Table S2.

Specific Annotation of Hermaphrodite and Male Data Clustered Together

To annotate our hermaphrodite and male integrated dataset, we used the markers identified in our male-only analysis to repeat the hypergeometric test. We also repeated the hypergeometric test and AUCell test with the original list of known markers for further confirmation. For sex-shared clusters where all tests aligned, we regarded this as the final annotation. For male-enriched clusters (>70% nuclei stemming from a male sample) where tests didn't agree, we deferred to the annotation based on the markers from the male-only data analysis. For hermaphrodite-enriched clusters, we deferred to our standard approach and manual curation of gold-standard markers. The results of all tests and the final annotation are summarized in supplemental (Table S3).

Hierarchical clustering

We used the normalized expression level of each gene in a given cluster to obtain average gene expression vectors, then calculated the Euclidean distance matrix between clusters. Lastly, we hierarchically clustered using the "hclust" function with the "complete" linkage method.

Threshold Setting for Expressed Genes

Similarly to CeNGEN[7] and St. Ange & Weng et al. 2024[19], we applied expression-level thresholds to the genes in our male-only dataset before assessing enrichment of a given gene in a particular cell type. We applied 4 thresholds that require a varying percent of expression of a gene within a cluster (0.5, 1, 1.5, or 3) and a minimum average normalized expression value (0.001) (Table S4). The same thresholds were applied to the hermaphrodite and male integrated dataset (Table S13).

Differential Gene Expression Analysis

Differential expression analysis was conducted as previously described[19]. Briefly, we used the FindMarkers function in the Seurat package and performed the Wilcoxon Rank Sum Test method on each neuron type, comparing male and hermaphrodite cells within the same cluster. Genes with a minimum percentage of expression in 10% of the cells were analyzed, and the significantly differentially expressed genes were identified if their $\log_2(FC) > 0.25$ or < -0.25, and adjusted p-value < 0.05.

Sexually dimorphic neurons that separated during unsupervised network clustering were merged into a singular Seurat object before differential expression. These neurons are the CEP/ADE/PDE, RMG, and PVW. We used the same statistical cutoffs for these neurons.

Comparison to Hermaphrodite Data

For comparison with the St. Ange and Weng et al dataset, we asked what genes were detected in our male-only dataset threshold 2 that were not detected in their WT N2 threshold 1 (least stringent). In this manner we were able to identify male-specific genes. To analyze sex-shared candidates, we compared the N2 WT threshold 2 with our male threshold 2. Since we cannot compare expression levels across these different genotypes, we simply asked what genes were detected in each cluster for each sex based on the 1% threshold. Only sex-shared neurons were analyzed in this case.

Gene Ontology Analysis

Upon comparing the male threshold 2 genes to the list of WT N2 threshold 1 genes, we identified a list of 693 male-enriched genes (Table S6). We then used g:Profiler[53] to perform functional enrichment analysis on this set of genes and chose significantly enriched molecular functions, biological processes, and/or cellular components (Bonferroni adjusted p-value < 0.05). Similarly, we identified PHD-enriched genes using the FindMarkers function in Seurat and performed functional enrichment using g:Profiler.

GFP reporter construction

Promoters upstream of the ATG start site of target genes were PCR amplified, and restriction enzyme cloned into the pPD95.75 Fire vector (Addgene). The promoter region for each construct was 5 kb upstream of the start site or up to the stop codon of the nearest coding gene, whichever criteria was met first. Promoter::GFP plasmids were injected into N2 animals at 25 ng/µL, with 1 ng/µL of *Pmyo3::mCherry* as a co-injection marker.

Fluorescent microscopy

Fluorescence microscopy was performed on the Nikon AXR confocal microscope using 60X magnification. Animals were synchronized and grown on HG plates until day 1. Day 1 animals were paralyzed with sodium azide on agar pads. We used 488 excitation to image our GFP reporters. Images were collected using a Z-stack with 0.4 uM increments. Images are processed with FIJI. Processing includes maximum intensity projection, brightness/contrasts adjusting, de-speckling, rotation, thresholding, splitting, and merging color channels. We evaluated expression of each construct in both sexes in at least 5 animals. Images were taken in regions where expression was observed, and 2-3 images were taken of hermaphrodites lacking expression of male-specific target genes. DiI staining was performed by adding 5uL of 2 mg/mL DiI into 1 mL of M9 and allowing animals to gently mix in this solution for 2 hrs prior to washing with M9, then imaging. Here we image using 488 and 561 excitation for GFP and mCherry.

Chemotaxis to female pheromone

Male pheromone preference assays were performed as previously described[18,54,55] using *sid-1* mutant males with pan-neuronal *sid-1* rescue for neuronal-specific knockdown upon RNAi treatment (described above). We used *C. remanei* true female pheromone since it has been shown to elicit a more robust response than *C. elegans* hermaphrodite pheromone[31,55]. *C. remanei* L4 females were picked onto freshly seeded NGM plates to ensure that they were unmated. Once females reach day 4, they were picked into M9 buffer with a concentration of 10 worms/100 µL M9. Animals are kept in M9 overnight to obtain a pheromone rich supernatant. The supernatant is then isolated for experiments. Pheromone may be kept at -20 °C for up to a month using single freeze-thaw cycles but works best fresh. For chemotaxis assays, 1 µL 7.5% sodium azide was added to each spot to paralyze the worms at each spot. Then, 2 µL of pheromone and M9 buffer control was spotted 5 cm apart on an unseeded 60 mm NGM plate. Males were washed 3x and 5 µL of lowly-dense pellet of males was added in-between the two spots. Then, males were given 1 hr to chemotaxis to either spot. Chemotaxis index is calculated as follows:

$$\text{Chemotaxis index (CI): } \frac{\#\text{ worms on pheromone} - \#\text{ worms on M9}}{Totat\ \#\ of\ worms - \#\ of\ worms\ at\ origin}\ x\ 100$$

Euclidean distance analysis

First the data was subset into each cluster, and further subset by sex (i.e. males and hermaphrodites) using the Seurat package. Only clusters categorized as sex-shared were analyzed, as marked by roughly ~30% or more nuclei from each sex present in that cluster. For males and hermaphrodites in each cluster, we generated a representative PC vector by averaging the column means of PCA embeddings from all cells in that cluster and genotype. Then, we calculated the Euclidean distance between the PC vector of male and hermaphrodite in each cluster. We ranked the distance from the largest to the smallest.

Quantification and statistics

Unpaired, two-tailed Student's t-test was performed to compare chemotaxis with only two conditions. Wilcoxon Rank Sum test's adjusted p-values are used for the identification of differentially expressed genes. Experiments were repeated on separate days, using separate independent populations, to confirm that results were reproducible. Prism 9 software was used for all statistical analyses. Software and statistical details used for RNA sequencing analyses are described in the method details section of the STAR Methods. Additional statistical details of experiments, including sample size (with n representing the number of chemotaxis assays performed for behavior, RNA collections for RNA-seq, and the number of worms for microscopy), can be found in the figure legends.

REFERENCES

1. Yang, C. F. *et al.* Sexually dimorphic neurons in the ventromedial hypothalamus govern mating in both sexes and aggression in males. *Cell* **153**, 896–909 (2013).
2. Oliveira-Pinto, A. V. *et al.* Sexual Dimorphism in the Human Olfactory Bulb: Females Have More Neurons and Glial Cells than Males. *PLOS ONE* **9**, e111733 (2014).
3. Jois, S., Chan, Y. B., Fernandez, M. P. & Leung, A. K.-W. Characterization of the Sexually Dimorphic fruitless Neurons That Regulate Copulation Duration. *Front. Physiol.* **9**, 780 (2018).
4. Bhattacherjee, A. *et al.* Cell type-specific transcriptional programs in mouse prefrontal cortex during adolescence and addiction. *Nat. Commun.* **10**, 4169 (2019).
5. Sex bias and omission in neuroscience research is influenced by research model and journal, but not reported NIH funding - ScienceDirect. https://www.sciencedirect.com/science/article/abs/pii/S0091302220300261.
6. Ferrandiz, N. *et al.* Spatiotemporal regulation of Aurora B recruitment ensures release of cohesion during C. elegans oocyte meiosis. *Nat. Commun.* **9**, 834 (2018).
7. Taylor, S. R. *et al.* Molecular topography of an entire nervous system. *Cell* **184**, 4329-4347.e23 (2021).
8. Barr, M. M., García, L. R. & Portman, D. S. Sexual Dimorphism and Sex Differences in Caenorhabditis elegans Neuronal Development and Behavior. *Genetics* **208**, 909–935 (2018).
9. Cook, S. J. *et al.* Whole-animal connectomes of both Caenorhabditis elegans sexes. *Nature* **571**, 63–71 (2019).

10. Walsh, J. D., Boivin, O. & Barr, M. M. What About the Males? The C. elegans Sexually Dimorphic Nervous System and a CRISPR-Based Tool to Study Males in a Hermaphroditic Species. *J. Neurogenet.* **34**, 323–334 (2020).

11. Luo, J., Barrios, A. & Portman, D. S. C. elegans males optimize mate-choice decisions via sex-specific responses to multimodal sensory cues. *BioRxiv Prepr. Serv. Biol.* 2023.04.08.536021 (2023) doi:10.1101/2023.04.08.536021.

12. Lipton, J., Kleemann, G., Ghosh, R., Lints, R. & Emmons, S. W. Mate Searching in Caenorhabditis elegans: A Genetic Model for Sex Drive in a Simple Invertebrate. *J. Neurosci.* **24**, 7427–7434 (2004).

13. Sakai, N. *et al.* A Sexually Conditioned Switch of Chemosensory Behavior in C. elegans. *PLOS ONE* **8**, e68676 (2013).

14. Lee, K. & Portman, D. S. Neural Sex Modifies the Function of a C. elegans Sensory Circuit. *Curr. Biol.* **17**, 1858–1863 (2007).

15. Fagan, K. A. *et al.* A Single-Neuron Chemosensory Switch Determines the Valence of a Sexually Dimorphic Sensory Behavior. *Curr. Biol.* **28**, 902-914.e5 (2018).

16. Wexler, L. R., Miller, R. M. & Portman, D. S. C. elegans Males Integrate Food Signals and Biological Sex to Modulate State-Dependent Chemosensation and Behavioral Prioritization. *Curr. Biol.* **30**, 2695-2706.e4 (2020).

17. Haque, R. *et al.* Sex-specific developmental gene expression atlas unveils dimorphic gene networks in C. elegans. *Nat. Commun.* **15**, 4273 (2024).

18. Weng, Y. & Murphy, C. T. Male-specific behavioral and transcriptomic changes in aging C. elegans neurons. *iScience* **27**, (2024).

19. Ange, J. St. *et al.* Adult Single-nucleus Neuronal Transcriptomes of Insulin Signaling Mutants Reveal Regulators of Behavior and Learning. Preprint at https://doi.org/10.1101/2024.02.07.579364 (2024).

20. Broverman, S. A. & Meneely, P. M. Meiotic Mutants That Cause a Polar Decrease in Recombination on the X Chromosome in Caenorhabditis Elegans. *Genetics* **136**, 119 (1994).

21. Ebert, M. S. & Bargmann, C. I. Evolution remodels olfactory and mating-receptive behaviors in the transition from female to hermaphrodite reproduction. *Curr. Biol.* **34**, 969-979.e4 (2024).

22. Sammut, M. *et al.* Glia-derived neurons are required for sex-specific learning in C. elegans. *Nature* **526**, 385–390 (2015).

23. Molina-García, L. *et al.* Direct glia-to-neuron transdifferentiation gives rise to a pair of male-specific neurons that ensure nimble male mating. *eLife* **9**, e48361 (2020).

24. The structure of the nervous system of the nematode *Caenorhabditis elegans*. *Philos. Trans. R. Soc. Lond. B Biol. Sci.* **314**, 1–340 (1986).

25. Poole, R. J., Flames, N. & Cochella, L. Neurogenesis in Caenorhabditis elegans. *Genetics* **228**, iyae116 (2024).

26. Wang, J. *et al.* Cell-Specific Transcriptional Profiling of Ciliated Sensory Neurons Reveals Regulators of Behavior and Extracellular Vesicle Biogenesis. *Curr. Biol.* **25**, 3232–3238 (2015).

27. Wang, C. *et al.* A neurotransmitter atlas of the nervous system of C. elegans males and hermaphrodites. *eLife* **13**, (2024).

28. Vidal, B. *et al*. An atlas of Caenorhabditis elegans chemoreceptor expression. *PLoS Biol*. **16**, e2004218 (2018).

29. Molina-García, L. *et al*. Direct glia-to-neuron transdifferentiation gives rise to a pair of male-specific neurons that ensure nimble male mating. *eLife* **9**, e48361.

30. Zahn, T. R., Macmorris, M. A., Dong, W., Day, R. & Hutton, J. C. IDA-1, a Caenorhabditis elegans homolog of the diabetic autoantigens IA-2 and phogrin, is expressed in peptidergic neurons in the worm. *J. Comp. Neurol*. **429**, 127–143 (2001).

31. SRD-1 in AWA neurons is the receptor for female volatile sex pheromones in C. elegans males. *EMBO Rep*. **20**, e46288 (2019).

32. LeBoeuf, B., Correa, P., Jee, C. & García, L. R. Caenorhabditis elegans male sensory-motor neurons and dopaminergic support cells couple ejaculation and post-ejaculatory behaviors. *eLife* **3**, e02938 (2014).

33. Barrios, A., Ghosh, R., Fang, C., Emmons, S. W. & Barr, M. M. PDF-1 neuropeptide signaling modulates a neural circuit for mate-searching behavior in C. elegans. *Nat. Neurosci*. **15**, 1675–1682 (2012).

34. Jarrell, T. A. *et al*. The Connectome of a Decision-Making Neural Network. *Science* **337**, 437–444 (2012).

35. Ebbing, A. *et al*. Spatial Transcriptomics of C. elegans Males and Hermaphrodites Identifies Sex-Specific Differences in Gene Expression Patterns. *Dev. Cell* **47**, 801-813.e6 (2018).

36. Beets, I. *et al*. System-wide mapping of peptide-GPCR interactions in C. elegans. *Cell Rep*. **42**, 113058 (2023).

37. Individual cell types in C. elegans age differently and activate distinct cell-protective responses: Cell Reports. https://www.cell.com/cell-reports/fulltext/S2211-1247(23)00913-0.

38. Spencer, W. C. *et al.* A spatial and temporal map of C. elegans gene expression. *Genome Res.* **21**, 325–341 (2011).

39. Oranth, A. *et al.* Food Sensation Modulates Locomotion by Dopamine and Neuropeptide Signaling in a Distributed Neuronal Network. *Neuron* **100**, 1414-1428.e10 (2018).

40. Packer, J. S. *et al.* A lineage-resolved molecular atlas of C. elegans embryogenesis at single-cell resolution. *Science* **365**, eaax1971 (2019).

41. McGrath, P. T. & Ruvinsky, I. A primer on pheromone signaling in Caenorhabditis elegans for systems biologists. *Curr. Opin. Syst. Biol.* **13**, 23–30 (2019).

42. Rogers, C. *et al.* Inhibition of Caenorhabditis elegans social feeding by FMRFamide-related peptide activation of NPR-1. *Nat. Neurosci.* **6**, 1178–1185 (2003).

43. Watteyne, J. *et al.* Neuromedin U signaling regulates retrieval of learned salt avoidance in a C. elegans gustatory circuit. *Nat. Commun.* **11**, 2076 (2020).

44. Gadenne, M. J. *et al.* Neuropeptide signalling shapes feeding and reproductive behaviours in male Caenorhabditis elegans. *Life Sci. Alliance* **5**, e202201420 (2022).

45. Nathoo, A. N., Moeller, R. A., Westlund, B. A. & Hart, A. C. Identification of neuropeptide-like protein gene families in Caenorhabditis elegans and other species. *Proc. Natl. Acad. Sci.* **98**, 14000–14005 (2001).

46. Li, C., Kim, K. & Nelson, L. S. FMRFamide-related neuropeptide gene family in Caenorhabditis elegans. *Brain Res.* **848**, 26–34 (1999).

47. Sengupta, P., Chou, J. H. & Bargmann, C. I. odr-10 Encodes a Seven Transmembrane Domain Olfactory Receptor Required for Responses to the Odorant Diacetyl. *Cell* **84**, 899–909 (1996).

48. Katanosaka, K., Takatsu, S., Mizumura, K., Naruse, K. & Katanosaka, Y. TRPV2 is required for mechanical nociception and the stretch-evoked response of primary sensory neurons. *Sci. Rep.* **8**, 16782 (2018).

49. Cabañero, D., Villalba-Riquelme, E., Fernández-Ballester, G., Fernández-Carvajal, A. & Ferrer-Montiel, A. ThermoTRP channels in pain sexual dimorphism: new insights for drug intervention. *Pharmacol. Ther.* **240**, 108297 (2022).

50. Brenner, S. The genetics of Caenorhabditis elegans. *Genetics* **77**, 71–94 (1974).

51. Kamath, R. S. & Ahringer, J. Genome-wide RNAi screening in Caenorhabditis elegans. *Methods San Diego Calif* **30**, 313–321 (2003).

52. Altun, Z. F. & Hall, D. H. Introduction to C. elegans Anatomy. in (WormAtlas., 2009).

53. Kolberg, L. *et al.* g:Profiler—interoperable web service for functional enrichment analysis and gene identifier mapping (2023 update). *Nucleic Acids Res.* **51**, W207–W212 (2023).

54. White, J. Q. *et al.* The Sensory Circuitry for Sexual Attraction in C. elegans Males. *Curr. Biol.* **17**, 1847–1857 (2007).

55. Shi, C., Runnels, A. M. & Murphy, C. T. Mating and male pheromone kill Caenorhabditis males through distinct mechanisms. *eLife* **6**, e23493 (2017).

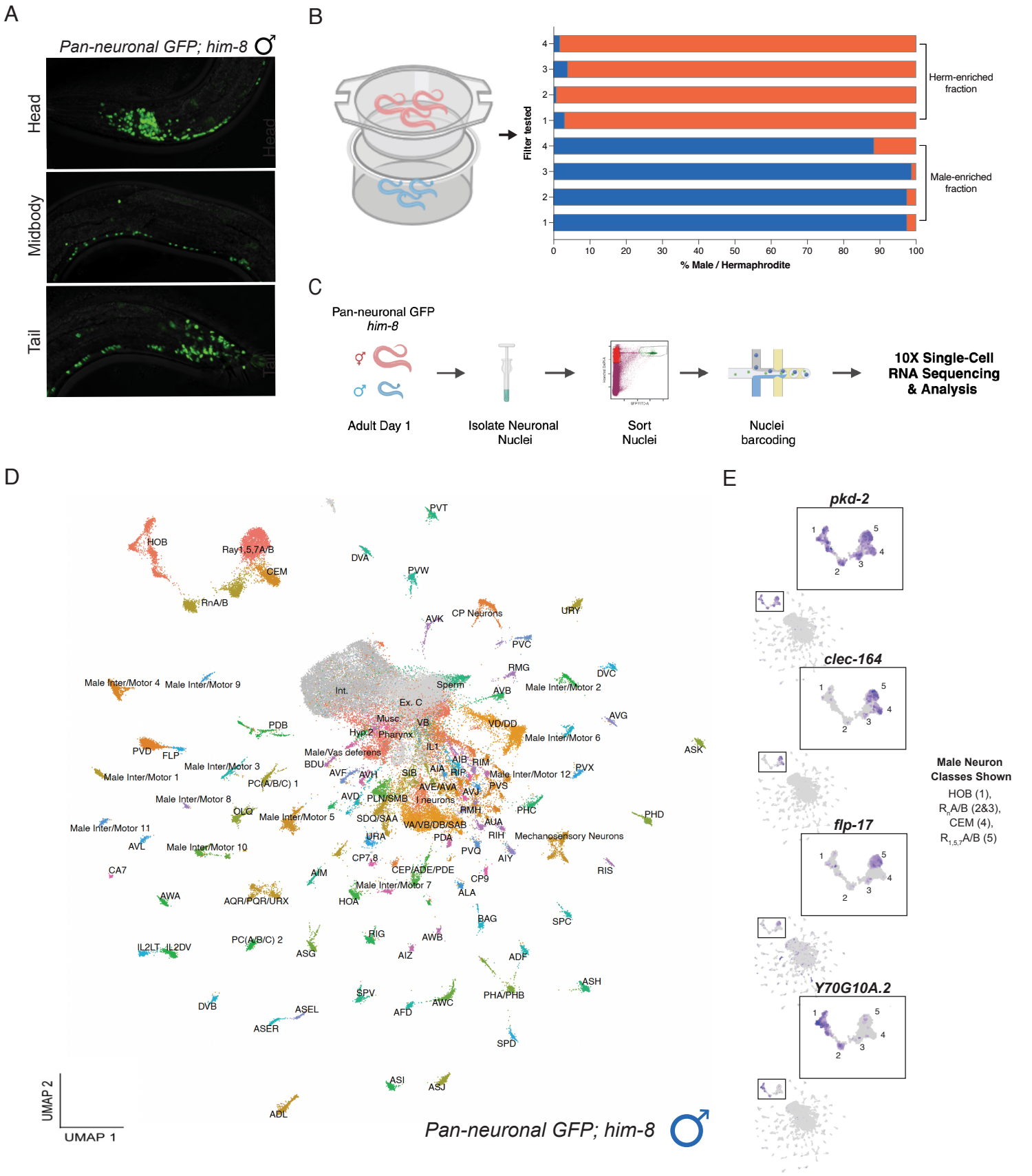
A
Pan-neuronal GFP; him-8 ♂
Head
Midbody
Tail
B
Filter tested
Herm-enriched fraction
Male-enriched fraction
% Male / Hermaphrodite
C
Pan-neuronal GFP
him-8
Adult Day 1
Isolate Neuronal Nuclei
Sort Nuclei
Nuclei barcoding
10X Single-Cell RNA Sequencing & Analysis
D
UMAP 2
UMAP 1
Pan-neuronal GFP; him-8 ♂
E
pkd-2
clec-164
flp-17
Y70G10A.2
Male Neuron Classes Shown
HOB (1),
R_nA/B (2&3),
CEM (4),
$R_{1,5,7}$A/B (5)

Figure 1

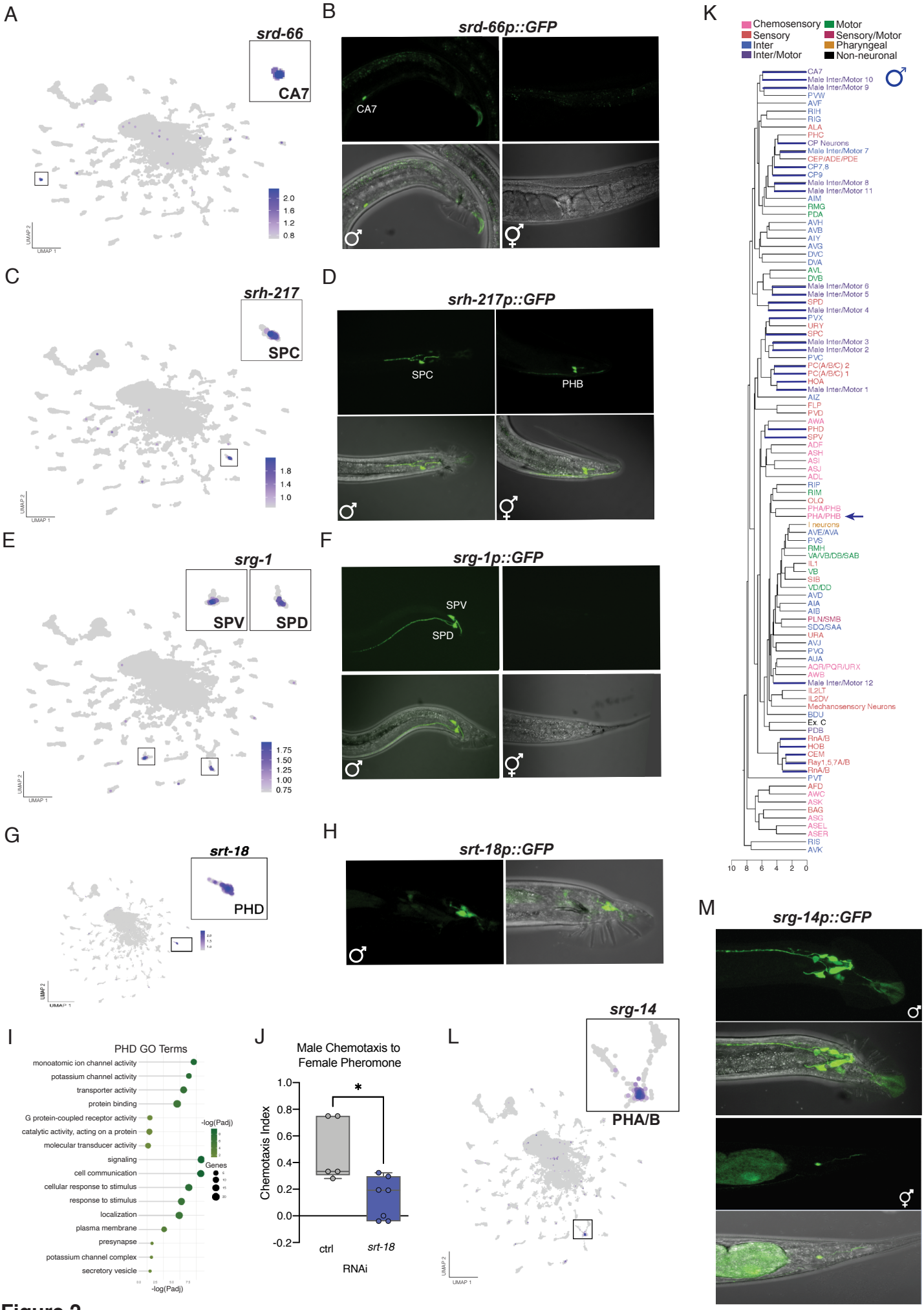
A
srd-66
CA7
2.0
1.6
1.2
0.8
UMAP 2
UMAP 1
B
srd-66p::GFP
CA7
C
srh-217
SPC
1.8
1.4
1.0
D
srh-217p::GFP
SPC
PHB
E
srg-1
SPV
SPD
1.75
1.50
1.25
1.00
0.75
F
srg-1p::GFP
SPV
SPD
G
srt-18
PHD
H
srt-18p::GFP
K
Chemosensory
Sensory
Inter
Inter/Motor
Motor
Sensory/Motor
Pharyngeal
Non-neuronal
CA7
Male Inter/Motor 10
Male Inter/Motor 9
PVW
AVF
RIH
RIG
ALA
PHC
CP Neurons
Male Inter/Motor 7
CEP/ADE/PDE
CP7,8
CP9
Male Inter/Motor 8
Male Inter/Motor 11
AIM
RMG
PDA
AVH
AVB
AIY
AVG
DVC
DVA
AVL
DVB
Male Inter/Motor 6
Male Inter/Motor 5
SPD
Male Inter/Motor 4
PVX
URY
SPC
Male Inter/Motor 3
Male Inter/Motor 2
PVC
PC(A/B/C) 2
PC(A/B/C) 1
HOA
Male Inter/Motor 1
AIZ
FLP
PVD
AWA
PHD
SPV
ADF
ASH
ASI
ASJ
ADL
RIP
RIM
OLQ
PHA/PHB
PHA/PHB
I neurons
AVE/AVA
PVS
RMH
VA/VB/DB/SAB
IL1
VB
SIB
VD/DD
AVD
AIA
AIB
PLN/SMB
SDQ/SAA
URA
AVJ
PVQ
AUA
AQR/PQR/URX
AWB
Male Inter/Motor 12
IL2LT
IL2DV
Mechanosensory Neurons
BDU
Ex. C
PDB
RnA/B
HOB
CEM
Ray1,5,7A/B
RnA/B
PVT
AFD
AWC
ASK
BAG
ASG
ASEL
ASER
RIS
AVK
10 8 6 4 2 0
M
srg-14p::GFP
I
PHD GO Terms
monoatomic ion channel activity
potassium channel activity
transporter activity
protein binding
G protein-coupled receptor activity
catalytic activity, acting on a protein
molecular transducer activity
signaling
cell communication
cellular response to stimulus
response to stimulus
localization
plasma membrane
presynapse
potassium channel complex
secretory vesicle
-log(Padj)
Genes
-log(Padj)
J
Male Chemotaxis to
Female Pheromone
Chemotaxis Index
1.0
0.8
0.6
0.4
0.2
0.0
-0.2
*
ctrl
srt-18
RNAi
L
srg-14
PHA/B

Figure 2

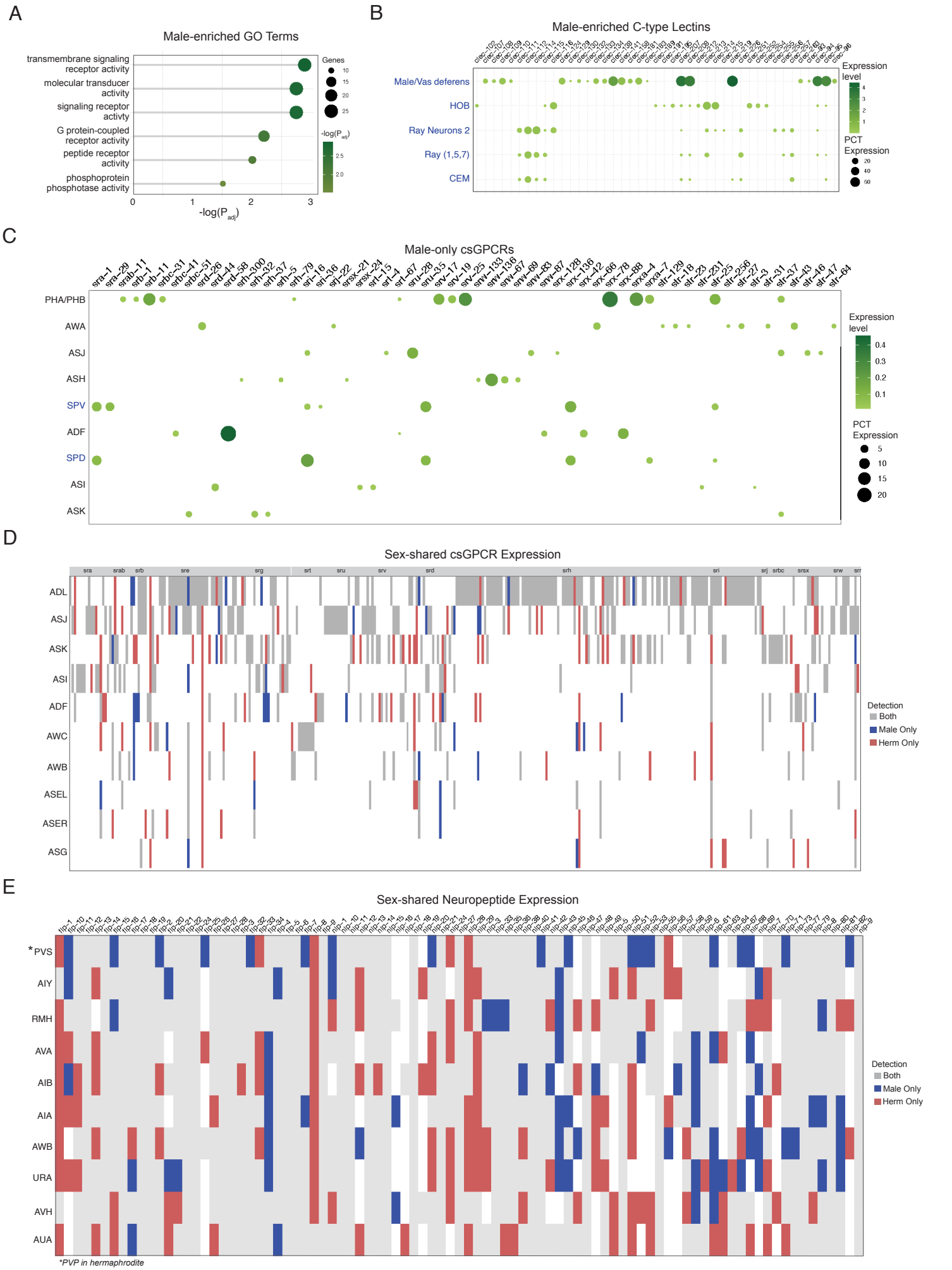
A
Male-enriched GO Terms
transmembrane signaling receptor activity
molecular transducer activity
signaling receptor activty
G protein-coupled receptor activity
peptide receptor activity
phosphoprotein phosphotase activity
-log(P_adj)
Genes
B
Male-enriched C-type Lectins
Male/Vas deferens
HOB
Ray Neurons 2
Ray (1,5,7)
CEM
Expression level
PCT Expression
C
Male-only csGPCRs
PHA/PHB
AWA
ASJ
ASH
SPV
ADF
SPD
ASI
ASK
Expression level
PCT Expression
D
Sex-shared csGPCR Expression
ADL
ASJ
ASK
ASI
ADF
AWC
AWB
ASEL
ASER
ASG
Detection
Both
Male Only
Herm Only
E
Sex-shared Neuropeptide Expression
*PVS
AIY
RMH
AVA
AIB
AIA
AWB
URA
AVH
AUA
Detection
Both
Male Only
Herm Only
*PVP in hermaphrodite

Figure 3

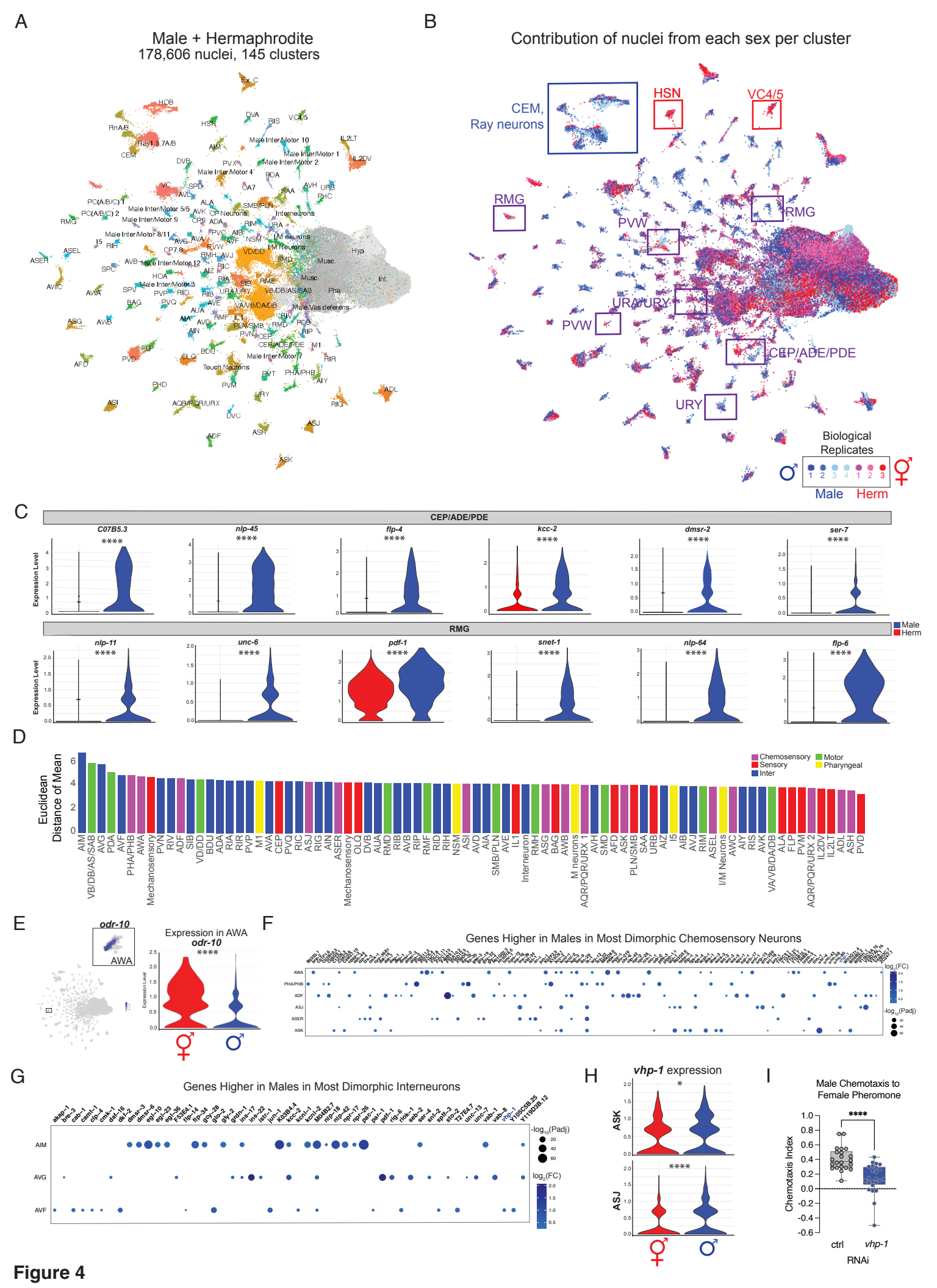
A
Male + Hermaphrodite
178,606 nuclei, 145 clusters
B
Contribution of nuclei from each sex per cluster
CEM, Ray neurons
HSN
VC4/5
RMG
PVW
URA/URY
CEP/ADE/PDE
URY
Biological Replicates
Male
Herm
C
CEP/ADE/PDE
C07B5.3
nlp-45
flp-4
kcc-2
dmsr-2
ser-7
RMG
nlp-11
unc-6
pdf-1
snet-1
nlp-64
flp-6
Expression Level
Male
Herm
D
Euclidean Distance of Mean
Chemosensory
Sensory
Inter
Motor
Pharyngeal
E
odr-10
AWA
Expression in AWA
odr-10
F
Genes Higher in Males in Most Dimorphic Chemosensory Neurons
G
Genes Higher in Males in Most Dimorphic Interneurons
H
vhp-1 expression
ASK
ASJ
I
Male Chemotaxis to Female Pheromone
Chemotaxis Index
ctrl
vhp-1
RNAi

Figure 4

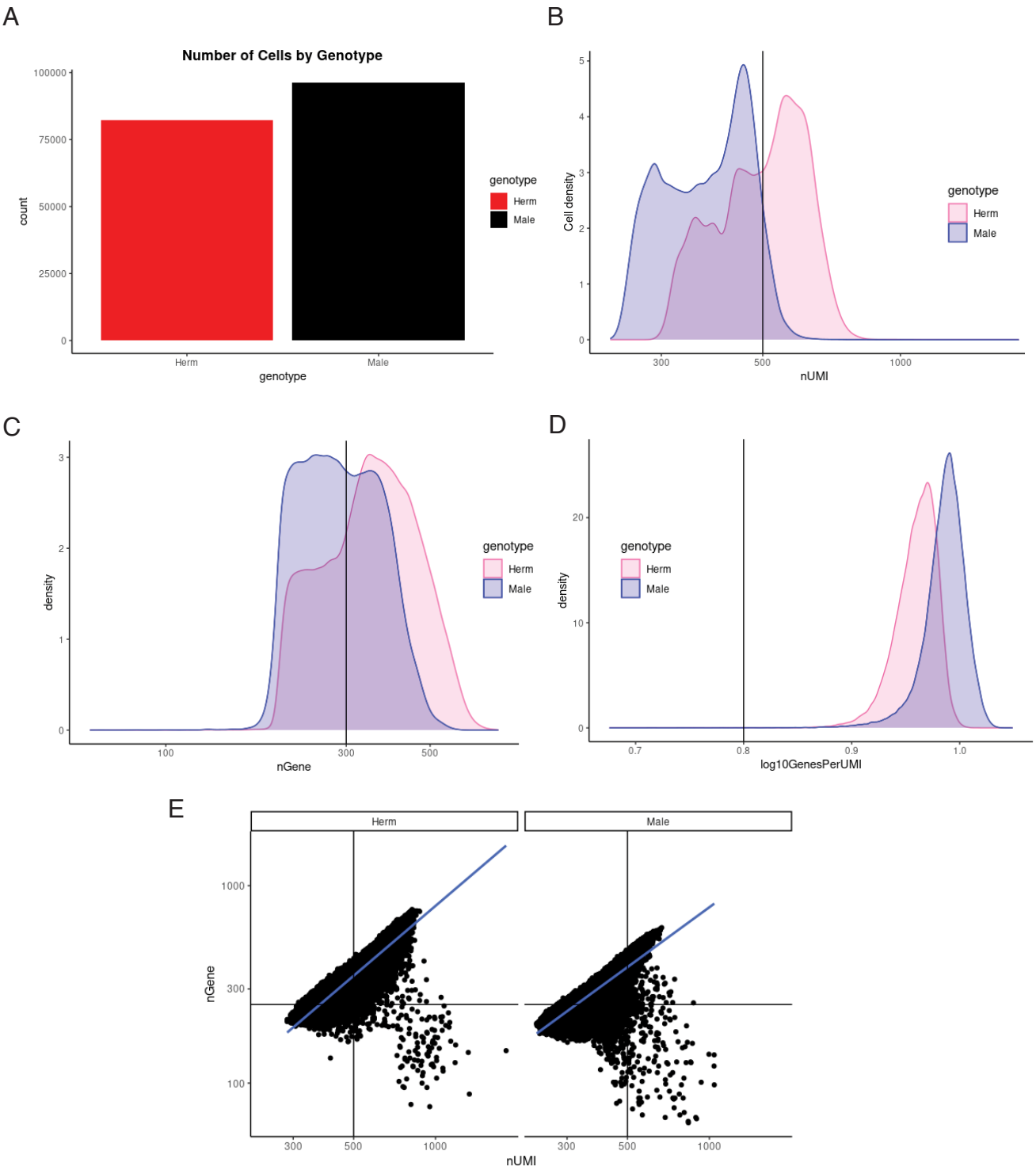

Supplementary Figure 1

A

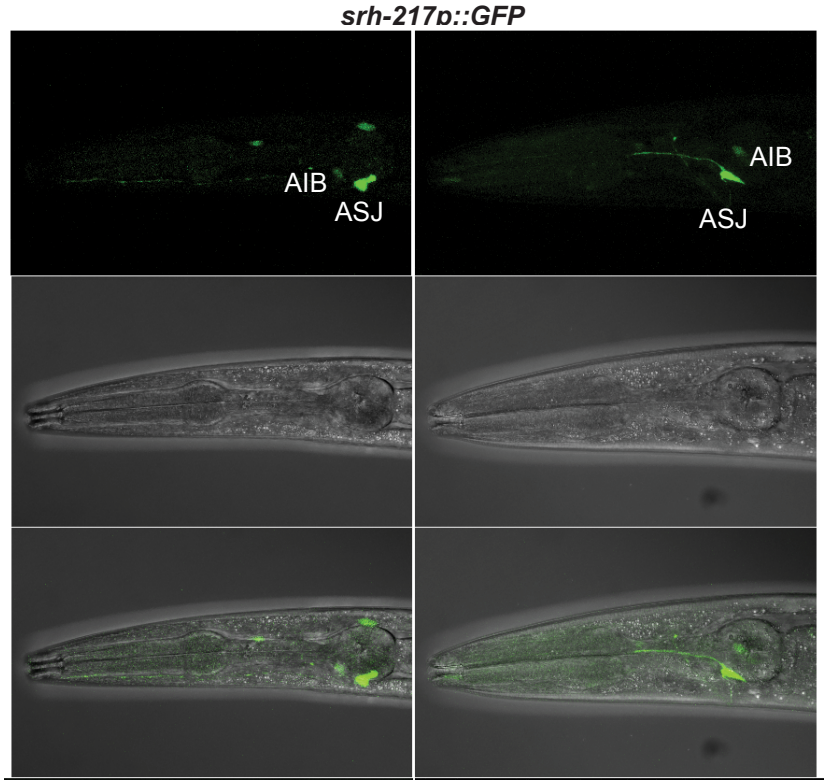

B

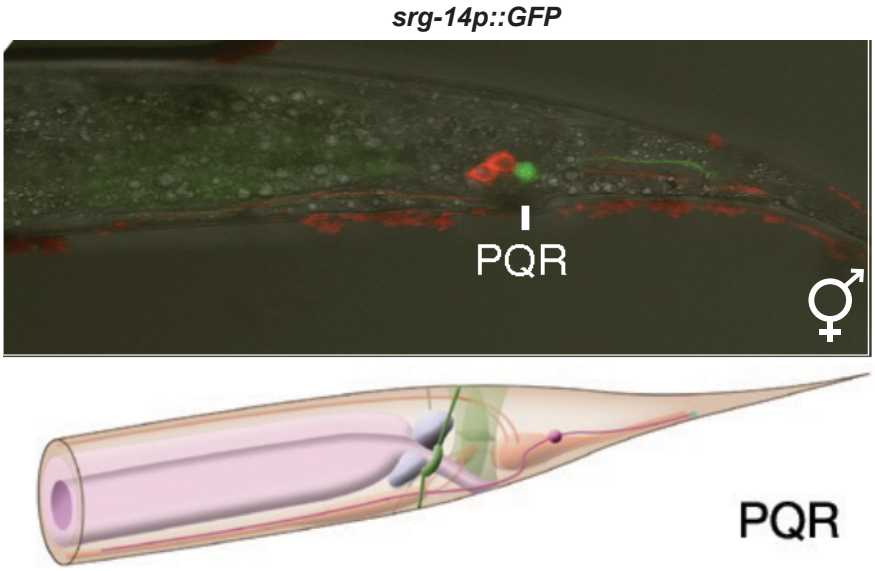

Supplementary Figure 2

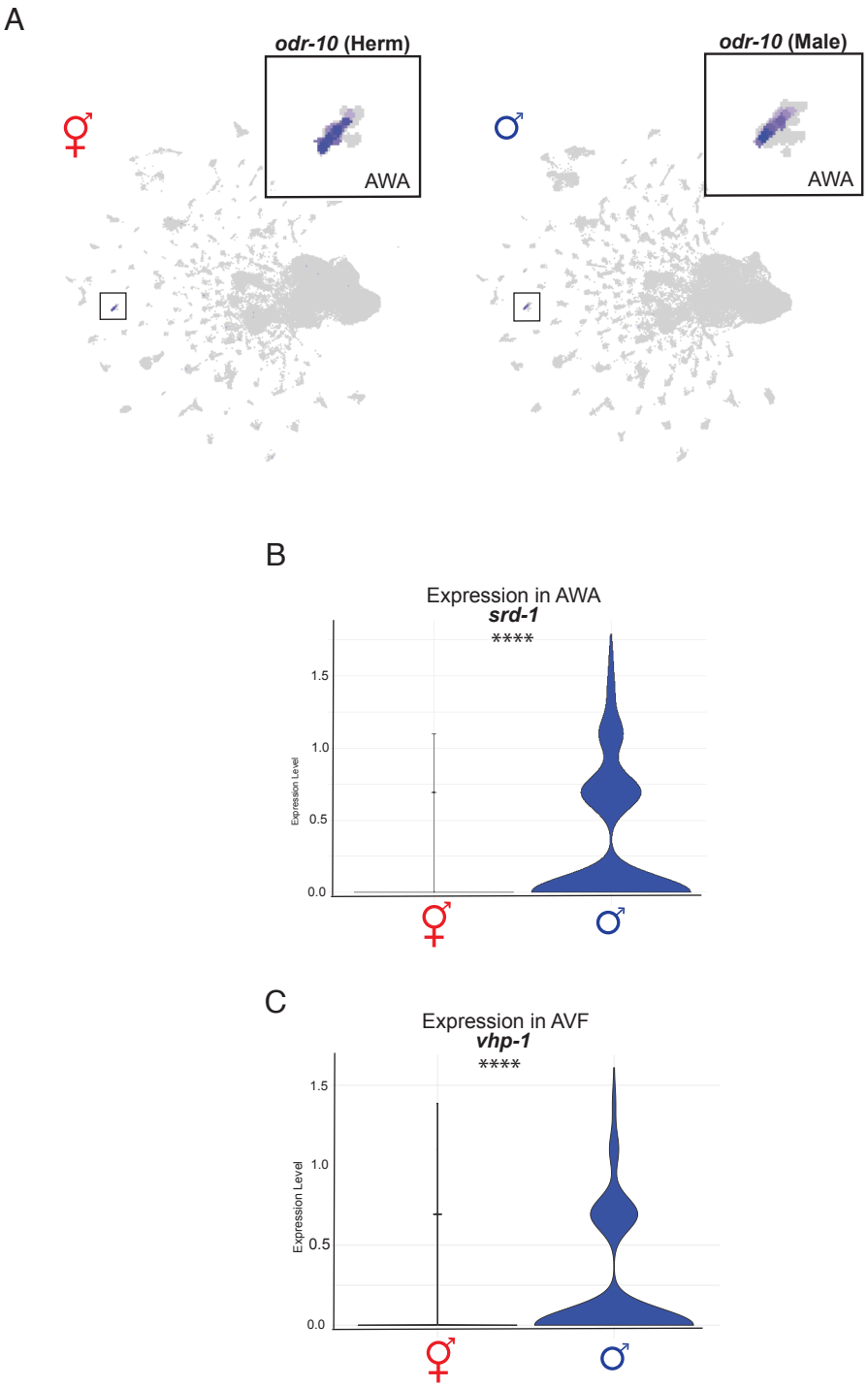

Supplementary Figure 3